Segmentation of Color Fundus Images of the Human Retina: Detection of the Optic Disc and the Vascular Tree Using Morphological Techniques

Thomas Walter and Jean-Claude Klein

Centre de Morphologie Mathématique, Ecole nationale supérieure des Mines de Paris
35 rue St.Honoré, 77305 Fontainebleau CEDEX, France
{walter,klein}@cmm.ensmp.fr
http://cmm.ensmp.fr/~walter/

Abstract. This paper presents new algorithms based on mathematical morphology for the detection of the optic disc and the vascular tree in noisy low contrast color fundus photographs. Both features – vessels and optic disc – deliver landmarks for image registration and are indispensable to the understanding of retinal fundus images. For the detection of the optic disc, we first find the position approximately. Then we find the exact contours by means of the watershed transformation. The algorithm for vessel detection consists in contrast enhancement, application of the morphological top-hat-transform and a post-filtering step in order to distinguish the vessels from other blood containing features.

1 Introduction

1.1 Outlines

In ophthalmology, the automatic detection of blood vessels as well as the detection of the optic disc may be of considerable interest for computer assisted diagnosis. Detecting and counting lesions in the human retina like microaneurysms and exudates is a time consuming task for ophthalmologists and open to human error. That is why much effort has been done to detect lesions in the human retina automatically. Finding the main components in the fundus images helps in characterizing detected lesions and in identifying false positives. Furthermore, vessel detection is interesting for the computation of parameters related to blood flow. The detection of the optic disc may be a first step in the early detection of the glaucoma. Over and above that, the optic disc and the vessels can be considered as landmarks of the fundus images, that may be used afterwards for image registration of images taken at different times or using different methods (as shown in [1]). To perform a robust feature based image registration, it is indispensable to rely on a robust and fast algorithm for vessel detection.

J. Crespo, V. Maojo, and F. Martin (Eds.): ISMDA 2001, LNCS 2199, pp. 282–287, 2001.

1.2 Some Morphological Operators

In this section we briefly define the basic morphological operators used in this paper (see [2], [3]).

Let $\mathcal{D}_f$ be a subset of $\mathbb{Z}^2$ and $T = \{t_{min}, ..., t_{max}\}$ be an ordered set of grey-levels. A grey-level image f can then be defined as a function $f : \mathcal{D}_f \subset \mathbb{Z}^2 \rightarrow T = \{t_{min}, ..., t_{max}\}$. Furthermore, let B be a subset of $\mathbb{Z}^2$ and $s \in \mathbb{N}$ a scaling factor, we can write the basic morphological operations as:

- Erosion: $\left[\varepsilon^{(sB)}(f)\right](x) = \min_{b \in sB} f(x+b)$
- Dilation: $\left[\delta^{(sB)}(f)\right](x) = \max_{b \in sB} f(x+b)$
- Opening: $\gamma^{(sB)}(f) = \delta^{(sB)}\left[\varepsilon^{(sB)}(f)\right]$
- Closing: $\phi^{(sB)}(f) = \varepsilon^{(sB)}\left[\delta^{(sB)}(f)\right]$

We call sB structuring element B of size s. Furthermore we may define the geodesic transformations of an image f (marker) and a second image g (mask):

- Geodesic erosion: $\varepsilon_g^{(n)}(f) = \varepsilon_g^{(1)}\varepsilon_g^{(n-1)}(f)$ with $\varepsilon_g^{(1)}(f) = \varepsilon^{(B)}(f) \vee g$
- Geodesic dilation: $\delta_g^{(n)}(f) = \delta_g^{(1)}\delta_g^{(n-1)}(f)$ with $\delta_g^{(1)}(f) = \delta^{(B)}(f) \wedge g$
- Opening by reconstruction: $\gamma_g^{rec}(f) = \delta_g^{(i)}(f)$ with $\delta_g^{(i)}(f) = \delta_g^{(i+1)}(f)$
- Closing by reconstruction: $\phi_g^{rec}(f) = \varepsilon_g^{(i)}(f)$ with $\varepsilon_g^{(i)}(f) = \varepsilon_g^{(i+1)}(f)$

2 Detection of the Optic Disc

2.1 Properties of the Optic Disc

The optic disc is the entrance of the vessels and the optic nerve into the retina. It appears in color fundus images as a bright yellowish or white region. Its shape is more or less circular, interrupted by the outgoing vessels. Sometimes it has the form of an ellipse because of a non-negligible angle between image plane and object plane. The size varies from patient to patient; its diameter lies between 40 and 60 pixels in 640×480 color photographs.

2.2 State of the Art

In [5] the optic disc is localized exploiting its high grey level variation. This approach has shown to work well, if there are no or only few pathologies like exudates, that also appear very bright and are also well contrasted. In [6] an area threshold is used to localize the optic disc. The contours are detected by means of the Hough transform. This approach is quite time consuming and it relies on conditions about the shape of the optic disc, that are not always met.

2.3 Algorithm Based on Morphological Operators

The Color Space Having compared several color spaces, we found the contours of the optic disc to appear most continuous and less disturbed by the outgoing vessels in the red channel f_r of the RGB color space. As this channel has a very small dynamic range and as we know that the optic disc belongs to the brightest parts of the color image, it is more reliable to work on the luminance channel f_l of the HLS color space to localize the optic disc and on f_r to find its contours.

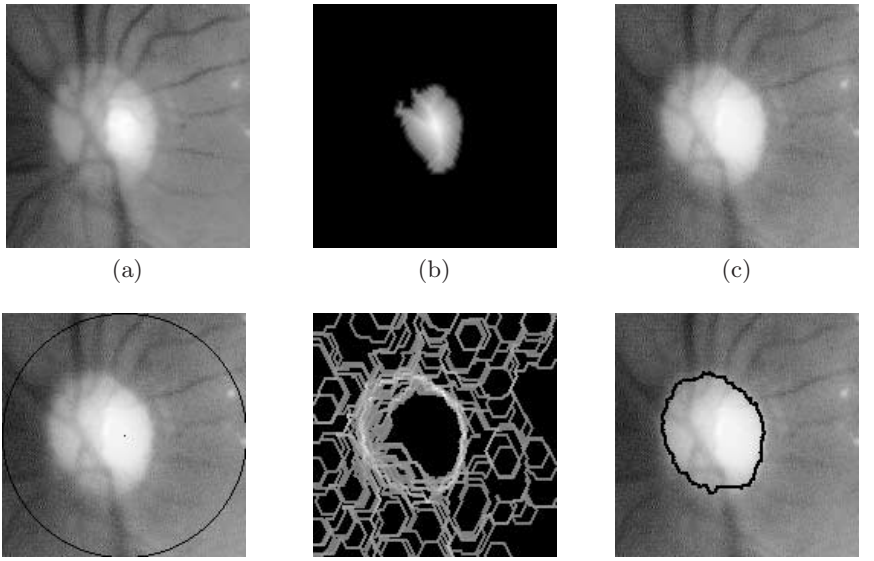

Fig. 1. The detection of the optic disc: (a) Luminance channel (b) Distance image of the biggest particle (c) red channel (d) red channel with imposed marker (e) morphological gradient (f) result of segmentation

Localizing the Optic Disc As we know approximately the size of the optic disc and as we can assume that parts of it belong to the brightest parts of the image f_l, we apply a simple area threshold to obtain a binary image b, that contains some parts of the optic disc as well as bright appearing pathologies like exudates. Exudates are not very big, and they are far from reaching the size of the optic disc. Hence, the biggest particle of the image b coincides with one part of the optic disc. Its centroid c , that can be calculated as the maximum of the discrete distance function of the biggest particle of b (shown in figure 1b) can be considered as an approximation for the locus of the optic disc.

In a first step we filter the image f_r in order to eliminate large gray level variations within the papillary region. First we "fill" the vessels, applying a simple closing $p_1 = \phi^{(s_1 B)}(f_r)$ with a hexagonal structuring element $s_1 B$ bigger than the maximal width of vessels. In order to remove large picks, we open the resulting image: $p_2 = \gamma^{(s_2 B)}(p_1)$. As this filter alters the shape of the papillary region considerably, we reconstruct it: $p_3 = \gamma_{p_1}^{rec}(p_2)$.

In order to detect the contours of the optic disc, we apply the classical watershed transformation [2] to the gradient $\Delta p_3 = \delta^{(B)} p_3 - \varepsilon^{(B)} p_3$ of the filtered image (shown in figure 1e) with c as internal marker and a circle among c with radius bigger than the diameter of the papilla as external marker (see figure 1d).

2.4 Results

We tested the algorithm on 30 color images of size 640×480 containing various pathologies. In all images, we could localize the optic disc with the proposed technique. In 27 images, we also found the exact contours. However, in some of the images, there were small parts missing or small false positives due to their low contrast. In 3 images the contrast was too low or the red channel too saturated, the algorithm failed and the result was not acceptable.

3 Detection of the Vascular Tree

3.1 Properties of the Vessels

Vessels appear darker than the background, their width is always smaller than a certain value λ, they are piecewise linear and they are connected in a tree like way. However these properties hold only approximately: Due to the presence of noise, the vessels are often disconnected, and not each pixel on a vessel appears darker than the background. The vessel borders appear often unsharp.

3.2 State of the Art

Much has been written about the detection of vessels in medical images; particularly for retinal images, matched filters [7], neuronal networks [5], a grouping algorithm of edgels [8] and a combination of linear and morphological methods [9] have been proposed. Our main objective is to conceive a fast and robust algorithm, the sensitivity being less important.

3.3 Vessel Detection Algorithm

In the following, we work on the green channel f_g of the RGB color space, because blood containing features appear most contrasted in this channel. In order to eliminate the noise and small "walls", that may disconnect the vascular tree, we apply a simple Gaussian filter, followed by an opening of size 2.

Now we apply $\vartheta g = TH\left[TM(g)\right]$ to the prefiltered image g, with the toggle-mapping $TM(g)$ (see [4])

$$h(x) = \left[TM(g)\right](x) = \begin{cases} \phi^{(s_1 B)} g(x) & \text{, if } \left[\phi^{(s_1 B)} g - g\right](x) \leq \left[g - \gamma^{(s_2 B)} g\right](x) \\ \gamma^{(s_2 B)} g(x) & \text{, if } \left[\phi^{(s_1 B)} g - g\right](x) > \left[g - \gamma^{(s_2 B)} g\right](x) \end{cases}$$

and the top-hat by closing $TH(h) = \phi^{(s_1 B)} h - h$ with s_1 equal for both operators. We choose s_1 in a way, that by applying $\phi^{(s_1 B)}$ the vessels are completely "filled". Therefore, the gray-level value $g(x)$ of a vessel pixel x is closer to the opening than to the closing, and so it will be darkened, whereas the border pixels will take the value of the closing (see figure 2). As $\phi^{(s_1 B)} h = \phi^{(s_1 B)} g$ (see [4]), all pixels that take the value of the closing in $TM(g)$, take a 0 in the top-hat-image, i.e. all holes extracted by the top-hat transform are disconnected.

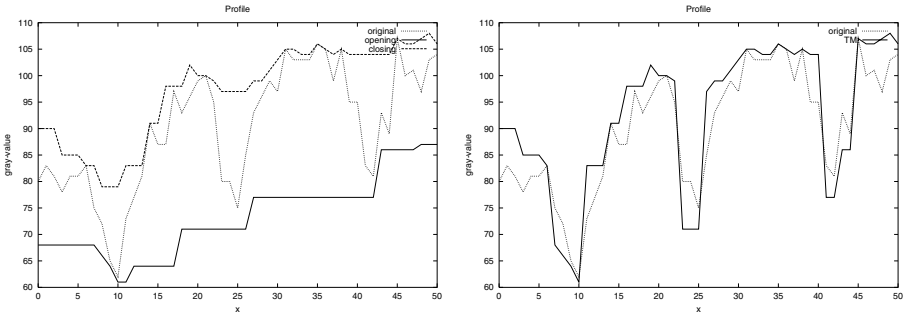

Fig. 2. The effect of the toggle-mappings: (a) shows a profile of an image with three vessels and the corresponding opening and closing (b) shows the resulting toggle-mapping

The rest is straightforward: Knowing that the vessels are piecewise linear we can calculate the supremum of openings with big linear structuring elements B_i (about 40 pixels) in different directions (we use the efficient recursive algorithms proposed in [2]). In that way we remove all features, into which the linear structuring element does not fit in any direction. As a result we obtain a set of unconnected lines. We can recover the vascular tree by an opening by reconstruction (for reconstruction operator see [2]):

$$\gamma^{sup}(\vartheta g) = \bigcup_{i=1}^{12} \gamma^{(sB_i)}(\vartheta g) \qquad R = \gamma_{\vartheta g}^{rec}[\gamma^{sup}(\vartheta g)]$$

3.4 Results

We tested the algorithm also on the 30 color images. The results are fully satisfactory in well contrasted images and still acceptable in low contrast images. Smaller vessels, if not connected to the rest of the vascular tree are often missed, which is not a drawback if vessel detection is used for image registration. There are very few false positives. However, if there are a lot of hemorrhages and microaneurysms, particularly if they are close to the vascular tree, another prefiltering step must be performed (an infimum of closings with linear structuring elements of different directions, followed by a closing by reconstruction, see [9]).

4 Conclusion

Two new algorithms for automatic segmentation of fundus images of the human retina have been presented in this paper. The optic disc and the vessels belong to the main features in the human eye, their detection is indispensable to understanding ocular fundus images. The proposed algorithms shall be used as a first step in image registration, for the identification of false positives in pathology detection and for classification of the detected pathologies.

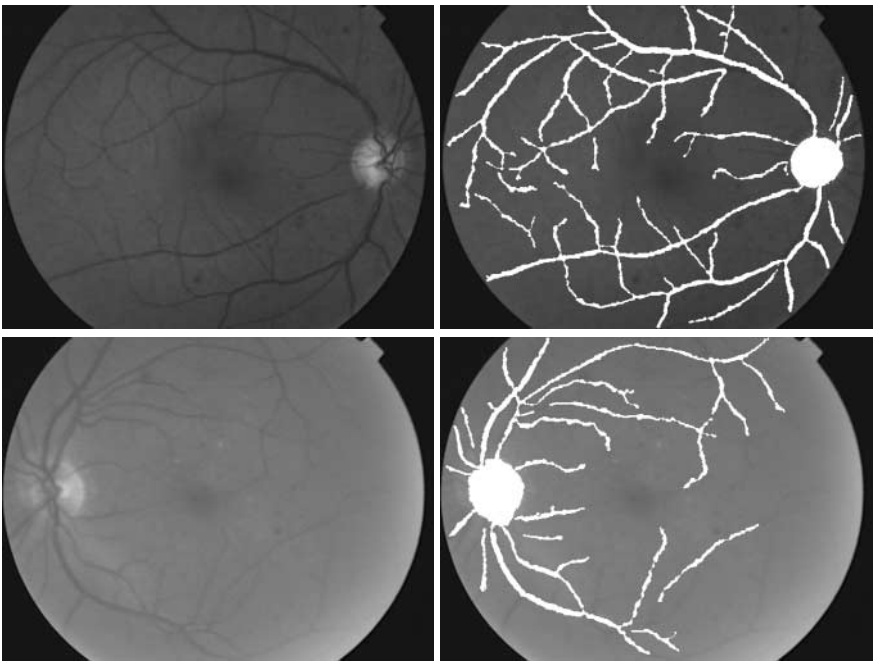

Fig. 3. The results of the segmentation algorithms

References

1. F. Zana and J.-C. Klein, A multi-modal segmentation algorithm of eye fundus images using vessel detection and hough transform, *IEEE Trans On Medical Imaging*, vol.18,no.5,1999. 282
2. P. Soille, *Morphological Image Analysis: Principles And Applications*, vol. 1, Springer-Verlag Berlin, Heidelberg, New York, 1999. 283, 284, 286
3. J. Serra, *Image analysis and mathematical morphology*, vol. 2, Academic Press, New York, 1988. 283
4. F. Meyer and J. Serra, Contrast and activity lattice, *Signal Processing*, vol. 16, no. 4, (303–317), 1989. 285
5. C. Sinthanayothin et al, Automated localisation of the optic disc, fovea and retinal blood vessels from digital colour fundus images, *British Journal of Ophtalmology*, vol. 83, no. 8, (231–238), 1999. 283, 285
6. S. Tamura et al, Zero-crossing interval correction in tracing eye-fundus blood vessels, *Pattern Recognition*, vol. 21, no. 3, (227–233), 1988. 283
7. S. Chaudhuri et al, Detection of blood vessels in retinal images using two-dimensional matched filters, *IEEE Trans On Medical Imaging*, vol. 8, no. 3, (263–269), 1989. 285
8. A. Pinz et al, Mapping the human retina, *IEEE Trans On Medical Imaging*, vol.1, no.1,(210–215),1998. 285
9. F. Zana and J.-C. Klein, Segmentation of vessel like patterns using mathematical morphology and curvature evaluation, *IEEE Trans On Medical Imaging*,2001, (to be published). 285, 286